Complexation of Polyoxometalates with Cyclodextrins

ARTICLE *in* JOURNAL OF THE AMERICAN CHEMICAL SOCIETY · MARCH 2015

Impact Factor: 12.11 · DOI: 10.1021/ja511713c

JACS
JOURNAL OF THE AMERICAN CHEMICAL SOCIETY
Article
pubs.acs.org/JACS

Complexation of Polyoxometalates with Cyclodextrins

Yilei Wu,[†] Rufei Shi,[†,∥] Yi-Lin Wu,[†] James M. Holcroft,[†] Zhichang Liu,[†] Marco Frasconi,[†] Michael R. Wasielewski,[†] Hui Li,*[,†,‡] and J. Fraser Stoddart*[,†]

[†]Department of Chemistry, Northwestern University, 2145 Sheridan Road, Evanston, Illinois 60208-3113, United States

[‡]Key Laboratory of Cluster Science of Ministry of Education, School of Chemistry, Beijing Institute of Technology, Beijing 100081, P. R. China

[∥]Department of Chemistry, Loras College, 1450 Alta Vista Street, Dubuque, Iowa 52001, United States

Supporting Information

ABSTRACT: Although complexation of hydrophilic guests inside the cavities of hydrophobic hosts is considered to be unlikely, we demonstrate herein the complexation between γ- and β-cyclodextrins (γ- and β-CDs) with an archetypal polyoxometalate (POM)—namely, the $[PMo_{12}O_{40}]^{3-}$ trianion—which has led to the formation of two organic–inorganic hybrid 2:1 complexes, namely $[La(H_2O)_9]\{[PMo_{12}O_{40}]\subset[\gamma\text{-CD}]_2\}$ (**CD-POM-1**) and $[La(H_2O)_9]\{[PMo_{12}O_{40}]\subset[\beta\text{-CD}]_2\}$ (**CD-POM-2**), in the solid state. The extent to which these complexes assemble in solution has been investigated by (i) ^{1}H, ^{13}C, and ^{31}P NMR spectroscopies and (ii) small- and wide-angle X-ray scattering, as well as (iii) mass spectrometry. Single-crystal X-ray diffraction reveals that both complexes have a sandwich-like structure, wherein one $[PMo_{12}O_{40}]^{3-}$ trianion is encapsulated by the primary faces of two CD tori through intermolecular [C–H···O═Mo] interactions. X-ray crystal superstructures of **CD-POM-1** and **CD-POM-2** show also that both of these 2:1 complexes are lined up longitudinally in a one-dimensional columnar fashion by means of [O–H···O] interactions. A beneficial nanoconfinement-induced stabilizing effect is supported by the observation of slow color changes for these supermolecules in aqueous solution phase. Electrochemical studies show that the redox properties of $[PMo_{12}O_{40}]^{3-}$ trianions encapsulated by CDs in the complexes are largely preserved in solution. The supramolecular complementarity between the CDs and the $[PMo_{12}O_{40}]^{3-}$ trianion provides yet another opportunity for the functionalization of POMs under mild conditions by using host–guest chemistry.

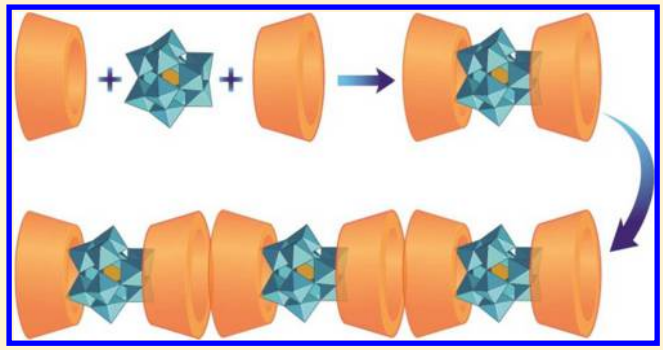

1. INTRODUCTION

Identifying organic and inorganic compounds that are capable of spontaneously self-assembling into hybrid systems[1] is one of the grand challenges in chemistry today. Engineering such hybrid assemblies with well-defined superstructures and emergent properties[2] can be a rewarding mission when it comes to producing new materials exhibiting properties not shared by their building blocks.

Polyoxometalates[3] (POMs) are discrete all-inorganic anionic metal–oxygen clusters (Figure 1a). Their wide structural diversity, along with their remarkable chemical and physical properties, have rendered them—given the fact that they are nanosized molecular clusters—useful for applications in areas ranging from materials science[4] and energy conversion[5] to catalysis[6] and medicine.[7] One of the major challenges that limits their wider exploitation is the development of robust and efficient synthetic protocols for their integration into hybrid architectures and devices. While most researchers investigating POMs have relied, in the past, on counterion exchange protocols as a general way to decorate these inorganic clusters with organic cations, more synthetically demanding covalent functionalization protocols are now emerging as a viable alternative for producing POM hybrids.[8] So far, the host–guest approach, which has the intrinsic advantages of providing (i) modular assembly, coupled with (ii) mild reaction conditions and (iii) error-checking capabilities, has remained under-explored.

Cyclodextrins[9] (CDs) are cyclic oligosaccharides comprised of six or more α-1,4-linked D-glucopyranosyl residues (Figure 1b). The shape-persistent hydrophobic cavities of these toroidal molecules allow encapsulation of suitable guests, and therefore they represent a class of receptors that are ideal for the construction of hybrid assemblies. Their exceptional inclusion capabilities[10] have led to their broad application in nanotechnology,[11] pharmaceutics,[12] medicine,[13] and environmental science.[14] Coordination of the primary and secondary hydroxyl groups of CDs to group IA metal cations has been exploited recently in the production of microporous CD-based metal–organic frameworks[15] (CD-MOFs), paving an alternative way toward the development of green and functional MOFs with

Received: November 21, 2014
Published: March 10, 2015

DOI: 10.1021/ja511713c
J. Am. Chem. Soc. 2015, 137, 4111–4118

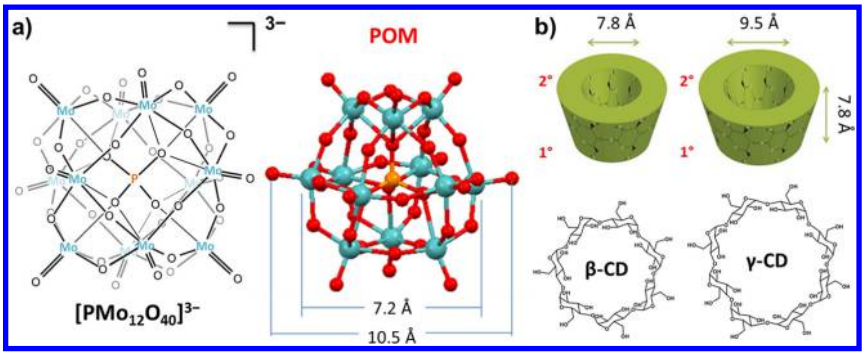

Figure 1. Structural formulas of (a) the $[PMo_{12}O_{40}]^{3-}$ trianion along with its X-ray crystal structure, and (b) β-CD and γ-CD. Color code: Mo, cyan; O, red; P, orange.

potential applications in gas storage, separation science, sensing, and catalysis.

In an attempt to assemble functional supramolecular hybrid architectures by installing an archetypal POM anion—namely, $[PMo_{12}O_{40}]^{3-}$—inside the micropores of CD-MOFs, we have uncovered the existence of a supramolecular association between CDs and a POM in aqueous solution as well as in the solid state. Structural analyses of these unprecedented[16] hybrid complexes have revealed the partial encapsulation of the anionic POMs in the inner cavities of CDs, in contradiction to the well-recognized belief that only hydrophobic compounds undergo association with CDs in aqueous solutions. The formation of the hybrid materials between native γ- and β-CD with the $[PMo_{12}O_{40}]^{3-}$ trianion—that is, $[La(H_2O)_9]\{[PMo_{12}O_{40}]\subset[\gamma\text{-CD}]_2\}$ (**CD-POM-1**) and $[La(H_2O)_9]\{[PMo_{12}O_{40}]\subset[\beta\text{-CD}]_2\}$ (**CD-POM-2**)—has been confirmed by (i) mass spectrometry (ESI-MS), (ii) ^{1}H NMR spectroscopy, and (iii) small- and wide-angle X-ray scattering (SAXS/WAXS) in the solution phase, while the solid-state superstructures have been characterized by (iv) powder and (v) single-crystal X-ray diffraction (XRD) analyses. Our findings draw attention to a host–guest approach to functionalizing POMs through noncovalent bonding interactions with readily available CDs.

2. EXPERIMENTAL SECTION

The full experimental details are provided in the Supporting Information. The most important experiments are described here.

2.1. CD-POM-1. A mixture of γ-CD (3.89 g, 3 mmol) and $H_3PMo_{12}O_{40}$ (2.74 g, 1.5 mmol) in deionized H_2O (20 mL) was stirred at room temperature until a clear yellow solution formed. This solution was filtrated to give solution A. A solution of $LaCl_3{\cdot}7H_2O$ (1.67 g, 4.5 mmol) in EtOH (8 mL) was added to solution A, and the resulting mixture was stirred at room temperature for 30 min. The crude product that precipitated was collected by filtration, washed with EtOH, and dried in air to afford the final product **CD-POM-1** (5.6 g, 79%). ^{1}H NMR (500 MHz, D_2O, ppm): δ = 5.05 (d, J = 3.9 Hz, 8 H), 4.11–4.01 (m, 24 H), 3.91 (d, J = 9.8 Hz, 8 H), 3.65–3.56 (m, 16 H). ^{13}C NMR (125 MHz, D_2O, ppm): δ = 102.6, 80.8, 72.9, 72.9, 71.9, 59.9.

2.2. CD-POM-2. A mixture of β-CD (1.13 g, 1 mmol) and $H_3PMo_{12}O_{40}$ (0.91 g, 0.5 mmol) in deionized H_2O (10 mL) was stirred at room temperature for 30 min. A solution of $LaCl_3{\cdot}7H_2O$ (0.56 g, 1.5 mmol) in H_2O (5 mL) was added to the first aqueous solution, and the resulting mixture was cooled (4 °C) in a refrigerator overnight. The yellow microcrystals that formed were collected by filtration, washed with EtOH, and dried in air to afford the final product **CD-POM-2** (1.6 g, 66%). ^{1}H NMR (500 MHz, D_2O, ppm): δ = 5.01 (d, J = 3.6 Hz, 7 H), 4.01–3.94 (m, 14 H), 3.90 (t, J = 9.5 Hz, 7 H), 3.75 (d, J = 9.9 Hz, 7 H), 3.65–3.51 (m, 14 H). ^{13}C NMR (125 MHz, D_2O, ppm): δ = 101.9, 81.3, 73.0, 72.1, 71.7, 59.8.

2.3. ^{1}H NMR Spectroscopy. ^{1}H NMR spectra were recorded at 298 K, unless otherwise stated, on a Bruker Avance III 500 MHz instrument. Chemical shifts are reported in ppm relative to the signals corresponding to the residual nondeuterated solvents (D_2O: δ_H = 4.79 ppm). All the ^{13}C NMR experiments were performed with simultaneous decoupling of ^{1}H nuclei.

2.4. ^{1}H NMR Titrations. ^{1}H NMR (298 K, 500 MHz) titrations were performed by adding small volumes of a concentrated POM solution in D_2O to a solution of CDs in D_2O. Tetramethylsilane was used as an internal reference. Significant upfield shifts of the ^{1}H resonances for the higher field H-6,6′ proton were observed and used to determine the association constants (K_a). For the complexation of POM with CDs, the K_a values were calculated using Dynafit, a program which employs nonlinear least-squares regression on receptor–substrate binding data.

2.5. Isothermal Titration Calorimetry (ITC). All ITC measurements were performed in degassed deionized H_2O at 298 K. An aqueous solution of $H_3PMo_{12}O_{40}$ was used as the guest solution in a 1.8 mL cell. Solutions of γ-CD (in H_2O) were added by injecting 10 μL of titrant successively over 20 s (25×), with a 300 s interval between injections. Experiments were repeated three times. Thermodynamic information was calculated using a two-site binding model, as well as a sequential binding model, utilizing data from which the heat of dilution of the host was subtracted, with the average of three runs being reported.

2.6. X-ray Scattering. SAXS/WAXS measurements were carried out at beamlines 12ID-C and 5ID-D at the Advanced Photon Source (APS), Argonne National Laboratory. Aqueous samples of $H_3PMo_{12}O_{40}$, γ-CD, and a mixture of $H_3PMo_{12}O_{40}$ (0.01 M) and γ-CD (0.1 M) were loaded into 2 mm quartz capillaries with a wall thickness of 0.2 mm. Scattering intensity is reported as a function of the modulus of the scattering vector q, related to the scattering angle 2θ by the equation $q = (4\pi/\lambda)\sin\theta$, where λ is the X-ray wavelength. At 12ID-C, the samples were examined by adjusting the sample-to-detector distance to measure across two detection ranges of q, 0.006–0.3 Å^{-1} and 0.1–1.6 Å^{-1}, whereas simultaneous data collection at 5ID-D over the wide q range made use of a Roper Scientific simultaneous SAXS/WAXS system. Subtracting the solvent scattering intensity ($I_{solvent}$) from the sample scattering (I_{sample}) gives the scattering contributed by the solute ($I_{solute} = I_{sample} - I_{solvent}$). For the mixture containing $H_3PMo_{12}O_{40}$ (0.01 M) and γ-CD (0.1 M), the contribution from γ-CD was further subtracted to give the scattering from the CD-POM complex.

2.7. Single-Crystal XRD Analyses. Single-crystal X-ray data were measured on a Bruker Kappa Apex II CCD diffractometer using Cu Kα radiation. Data collection and structure refinement details can be found in the SI, including the CIF files. CCDC 963487 and 963488 also contain the supplementary crystallographic data for this paper. These data can be obtained free of charge via www.ccdc.cam.ac.uk/data_request/cif.

DOI: 10.1021/ja511713c
J. Am. Chem. Soc. 2015, 137, 4111–4118

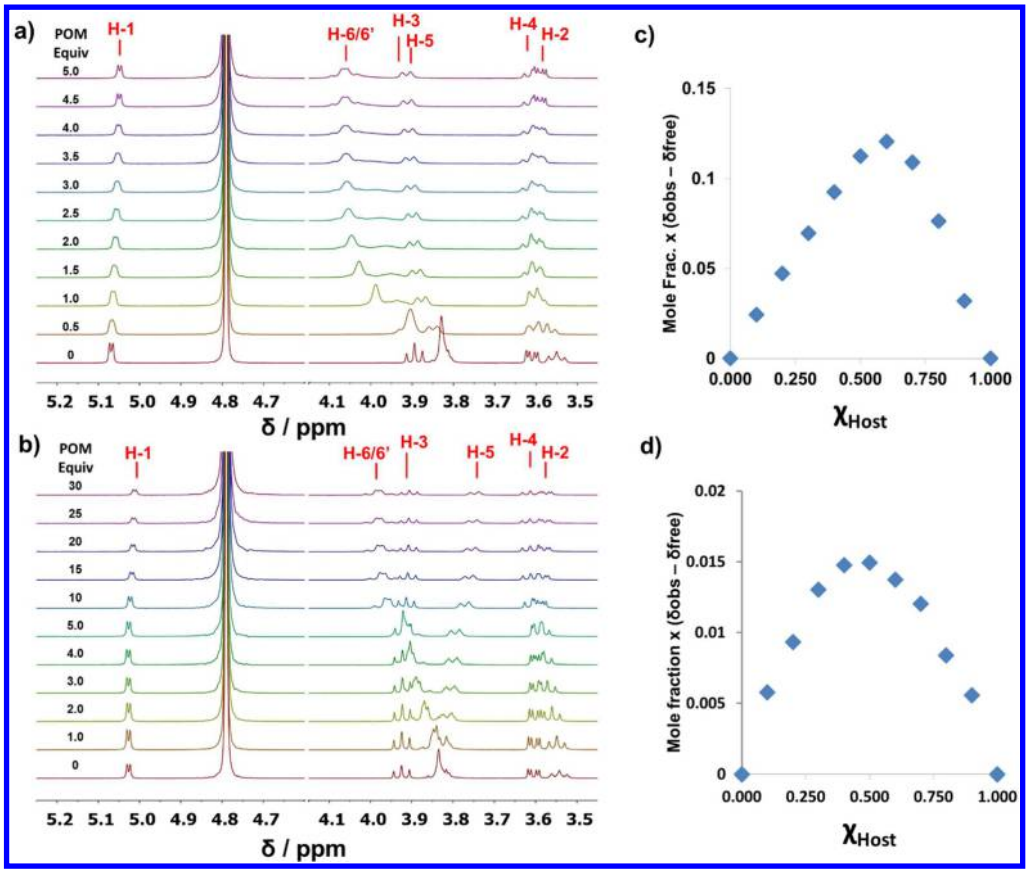

Figure 2. Partial ^{1}H NMR spectra (500 MHz, 298 K, D_2O, 1 mM) of (a) γ-CD and (b) β-CD in the presence of the $[PMo_{12}O_{40}]^{3-}$ trianion at different concentrations. The significant shifts of inner-surface protons H-5 and the primary face protons (H-6/6′), which are observed in both cases, suggest that the POM is inserted into the cavities of γ-CD and β-CD at their primary faces. Job plots between (c) γ-CD and (d) β-CD with $[PMo_{12}O_{40}]^{3-}$ trianion were obtained by plotting the chemical shift changes of the γ-CD and β-CD H-6/6′ protons (high-field signal) against the molar fraction of the $[PMo_{12}O_{40}]^{3-}$ trianion.

2.8. $[La(H_2O)_9]\{[PMo_{12}O_{40}]\subset[\gamma\text{-CD}]_2\}$ (CD-POM-1). *Method.* Single crystals suitable for X-ray crystallograpy were grown by liquid/liquid diffusion. A solution (4 mL) of γ-CD (38.9 mg, 0.03 mmol) and $LaCl_3{\cdot}7H_2O$ (16.7 mg, 0.045 mmol) in deionized H_2O was added to the bottom of a 10 mL test tube. A solution (5 mL) of $H_3PMo_{12}O_{40}$ (27.4 mg, 0.015 mmol) in EtOH was then added carefully to the test tube along the walls, keeping the interface between the two solutions clear. Single crystals of **CD-POM-1** were obtained after slow diffusion during 1 week. Data were collected at 100 K on a Bruker Kappa APEX2 CCD diffractometer equipped with a Cu Kα microsource with Quazar optics. SADABS-2008 was used for absorption correction. $wR_{2(int)}$ was 0.0813 before and 0.0512 after correction. The ratio of minimum to maximum transmission was 0.6940. The $\lambda/2$ correction factor was 0.0015.

Crystal Parameters. $[La(H_2O)_9][C_{48}H_{80}O_{40}]_2[PMo_{12}O_{40}]$, M_r = 4699.39; green block (0.347 × 0.292 × 0.204 mm); orthorhombic, space group $P2_12_12$ (no. 18); a = 23.5194(8), b = 24.5275(8), and c = 18.4585(7) Å; V = 10 648.2(6) Å^3; T = 100 K; Z = 2; μ(Cu Kα) = 8.026; 76 047 reflections measured, 18 677 unique (R_{int} = 0.0356) which were used in all calculations; final R_1 = 0.0891 (all data) and wR_2 = 0.2374. CCDC number: 963487.

2.9. $[La(H_2O)_9]\{[PMo_{12}O_{40}]\subset[\beta\text{-CD}]_2\}$ (CD-POM-2). *Methods.* Single crystals suitable for X-ray crystallograpy were grown by slow vapor diffusion. A solution of β-CD (3.39 mg, 3 μmol), $H_3PMo_{12}O_{40}$ (2.73 mg, 1.5 μmol), and $LaCl_3{\cdot}7H_2O$ (1.68 mg, 4.5 μmol) in deionized H_2O (1 mL) was filtered through a 0.45 μm filter into three 1 mL tubes. The tubes were inserted into a 20 mL vial containing Me_2CO (6 mL), and the vial was capped. Single crystals of **CD-POM-2** were obtained after 1 week. Data were collected at 100 K on a Bruker Kappa Apex2 CCD area detector equipped with a Mo Kα sealed tube with graphite. SADABS-2008 was used for absorption correction. $wR_{2(int)}$ was 0.0835 before and 0.0736 after correction. The ratio of minimum to maximum transmission was 0.9332. The $\lambda/2$ correction factor was 0.0015.

Crystal Parameters. $[La(H_2O)_9][C_{42}H_{70}O_{35}]_2[PMo_{12}O_{40}]{\cdot}27H_2O$, M_r = 4825.25; monoclinic, space group $P2_1$ (no. 4); a = 15.2351(7), b = 42.456(2), and c = 15.4011(7) Å; β = 101.763(2)°; V = 9752.5(8) Å^3; T = 100 K; Z = 2; μ(Mo Kα) = 1.079; 161 017 reflections measured, 39 978 unique (R_{int} = 0.0685) which were used in all calculations; final R_1 = 0.0529 (all data) and wR_2 = 0.1308. CCDC number: 963488.

2.10. Electrochemistry. Cyclic voltammetry (CV) experiments were carried out at room temperature in argon-purged solutions of DMF with a Gamry Multipurpose instrument interfaced to a PC. All CV experiments were performed using a glassy carbon working electrode (0.071 cm^2). The electrode surface was polished routinely with an 0.05 μm alumina−water slurry on a felt surface immediately before use. The counter electrode was a Pt coil, and the reference electrode was a Ag/AgCl electrode.

3. RESULTS AND DISCUSSION

3.1. Synthesis. The formation of complexes between the $[PMo_{12}O_{40}]^{3-}$ trianion and the CDs in aqueous solution was readily achieved by mixing 2 equiv of the CDs, dissolved in deionized water, with an aqueous solution of 1 equiv of $H_3[PMo_{12}O_{40}]$ at a concentration of ca. 0.1 M with respect to the CDs. The solid-state complex **CD-POM-1** was obtained by co-crystallization of a mixture of $LaCl_3{\cdot}7H_2O$, $H_3[PMo_{12}O_{40}]$, and γ-CD by liquid/liquid (H_2O/EtOH) diffusion, while the

DOI: 10.1021/ja511713c
J. Am. Chem. Soc. 2015, 137, 4111−4118

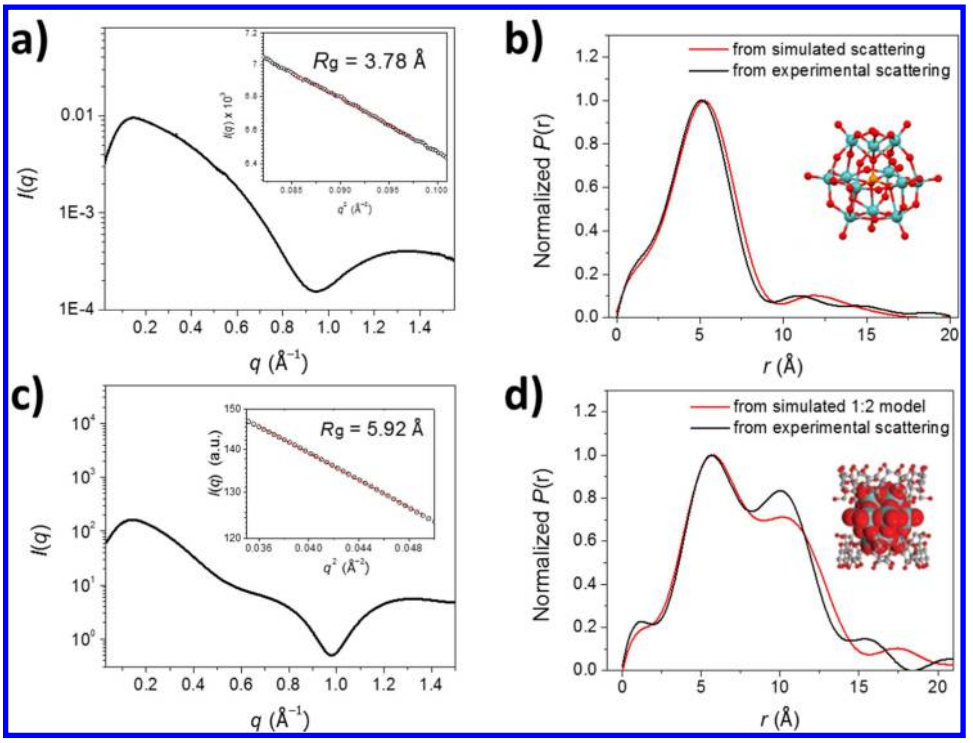

Figure 3. SAXS/WAXS data of (a) the sample containing the $[PMo_{12}O_{40}]^{3-}$ trianion (0.01 M) and (c) the sample containing the $[PMo_{12}O_{40}]^{3-}$ trianion (0.01 M) and γ-CD (0.1 M) in H_2O. Insets show the Guinier fit of the SAXS data; radius of gyration R_g = 3.78 and 5.92 Å for the $[PMo_{12}O_{40}]^{3-}$ trianion and the $[PMo_{12}O_{40}]^{3-}\subset[\gamma\text{-CD}]_2$ complex, respectively. Comparison of the pair distance distribution functions (PDFs) generated from the experimental scattering data (black lines) with that from the simulated structural model (red lines) for (b) the $[PMo_{12}O_{40}]^{3-}$ trianion and (d) the $[PMo_{12}O_{40}]^{3-}\subset[\gamma\text{-CD}]_2$ complex.

solid-state complex **CD-POM-2** was prepared by slow vapor diffusion of Me_2CO into an aqueous solution of a mixture of $LaCl_3{\cdot}7H_2O$, $H_3[PMo_{12}O_{40}]$, and β-CD.

3.2. ^{1}H NMR Titration. The formation of inclusion complexes in solution between CDs and the $[PMo_{12}O_{40}]^{3-}$ trianion was probed by concentration-dependent ^{1}H NMR spectroscopy. Upon increasing the concentration of the trianion in D_2O solutions of γ-CD (Figure 2a) and β-CD (Figure 2b), ^{1}H NMR spectra showed significant chemical shift changes in the resonances for the inner-cavity H-5 protons and the H-6/6′ protons on the primary faces of the CD tori. This observation suggests that the trianion interacts with the primary faces of these CDs and that it is embedded deeply enough to develop a shielding tensor of sufficient size which influences the chemical shifts of the H-5 proton resonances. Job plot analyses reveal that γ-CD forms a 2:1 complex with the $[PMo_{12}O_{40}]^{3-}$ trianion (Figure 2c), while in the case of β-CD, a 1:1 complex is the dominant one in aqueous solution (Figure 2d). The chemical shift changes of the signals for ^{13}C and ^{31}P nuclei are also observed in the ^{13}C and ^{31}P NMR spectra, respectively (Figures S11 and S12). These changes are small, reflecting complexation-induced conformational changes on the part of the CDs and $[PMo_{12}O_{40}]^{3-}$ trianion.

3.3. Isothermal Titration Calorimetry. In order to determine the binding strengths of the complexes formed between the CDs and the $[PMo_{12}O_{40}]^{3-}$ trianion, ITC experiments were performed. The ITC data (Figure S13), along with the ^{1}H NMR spectroscopic results, indicate that the formation of the 2:1 inclusion complex between γ-CD and the $[PMo_{12}O_{40}]^{3-}$ trianion is characterized by two-step sequential binding modes with K_1 and K_2 = 4.04 × 10^4 and 1.18 × 10^3 M^{-1}, respectively. By contrast, the binding affinity between the smaller β-CD and the $[PMo_{12}O_{40}]^{3-}$ trianion is found to be weaker (K = 1.97 × 10^3 M^{-1}) than that involving γ-CD.[17]

3.4. Small- and Wide-Angle X-ray Scattering. In order to elucidate the structure of these supramolecular assemblies in solution phase, SAXS/WAXS measurements were carried out. The experimental scattering data reveal the superstructures at a resolution of a few Ångstroms. A sample of $H_3PMo_{12}O_{40}$ was first tested to evaluate the applicability of the SAXS/WAXS technique on the POM-based systems. Figure 3a shows a plot of the logarithm of the scattering intensity $[I(q)]$ versus the scattering vector (q). A minimum can be observed around $q \approx$ 0.94 $Å^{-1}$, with a downturn at low q (<0.2 $Å^{-1}$). The latter feature, mainly caused by the structure factor of the system,[18] reflects the repulsive electrostatic interparticle interactions between the $[PMo_{12}O_{40}]^{3-}$ trianionic clusters in concentrated aqueous solutions. The theoretical scattering of this cluster was simulated by SolX,[19] and both the experimental and simulated scattering at q = 0−1.5 $Å^{-1}$ were Fourier transformed using GNOM[20] to give the real-space information in the atomic pair distance distribution function (PDF). PDFs, calculated on the basis of the experimental and simulated scattering, both exhibit the highest probabilities at r = 5.1 Å (Figure 3b). The high resemblance between the two PDFs indicates that the recorded SAXS/WAXS scattering intensity can be explained well by the Keggin structure of this POM.

The scattering of the sample containing $[PMo_{12}O_{40}]^{3-}$ trianion (0.01 M) and γ-CD (0.1 M) is shown in Figure 3c. The presence of excess γ-CD is to ensure 100% population of the complexed trianion. A sample constituted of $[PMo_{12}O_{40}]^{3-}$ (0.01 M) and 0.02 M γ-CD was also examined and produced a similar scattering response (Figure S6). As in the case of the $[PMo_{12}O_{40}]^{3-}$ trianion, a minimum of scattering intensity was

DOI: 10.1021/ja511713c
J. Am. Chem. Soc. 2015, 137, 4111−4118

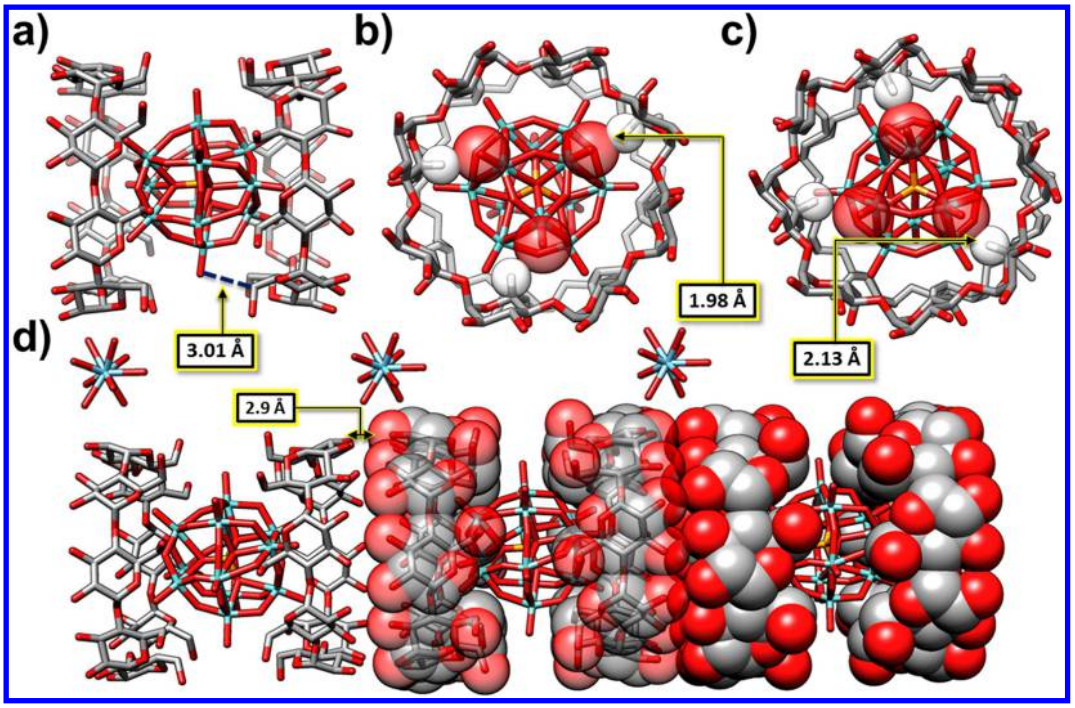

Figure 4. Capped-stick representations of the solid-state superstructure of **CD-POM-1**: (a) side-on view, (b) top plan view, and (c) bottom plan view. (d) Progression, from left to right, of a tubular to a space-filling representation of the solid-state superstructure of the **CD-POM-1** complexes, showing the aligned one-dimensional tubular stacks of the complexes and the intermolecular (O···O) distances between CDs of ca. 2.9 Å. Color code: Mo, cyan; La, blue; O, red; C, gray; P, orange; H, white. Hydrogen atoms except for those involved in [C−H···O] interactions have been omitted for the sake of clarity.

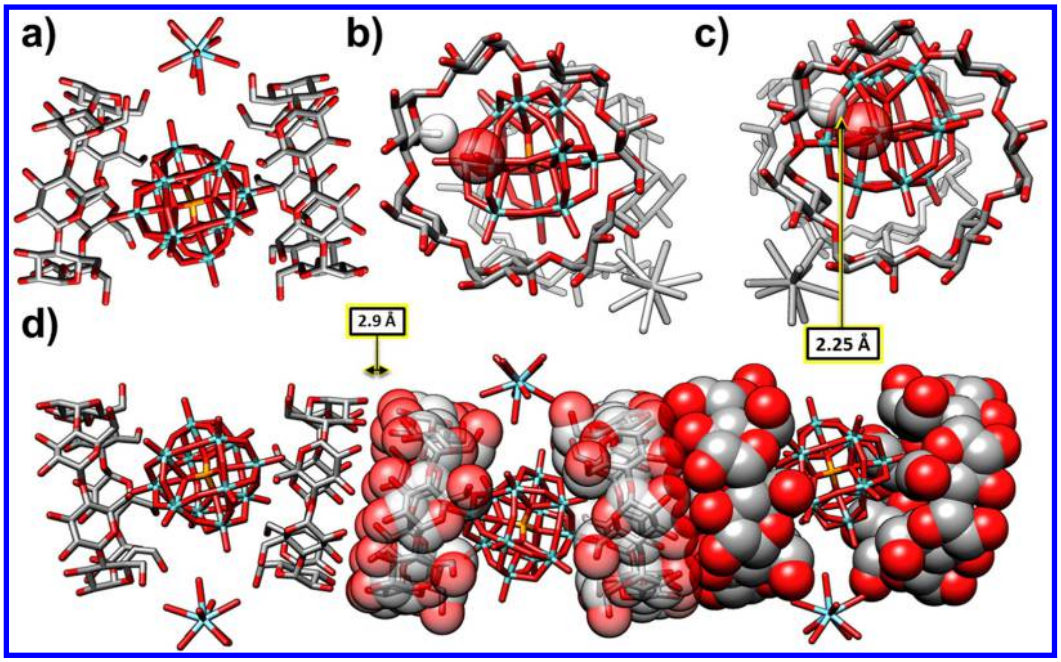

Figure 5. Capped-stick representations of the solid-state superstructure of **CD-POM-2**: (a) side-on view, (b) top plan view, and (c) bottom plan view. (d) Progression, from left to right, of a tubular to a space-filling representation of the solid-state superstructure of the **CD-POM-2** complex, showing the "zig-zag"-shaped one-dimensional tubular stacks of the complexes and the intermolecular (O···O) distances between CDs of ca. 2.9 Å. Color code: Mo, cyan; La, blue; O, red; C, gray; P, orange; H, white. The hydrated $La(H_2O)_9]^{3+}$ countercations in the solid state are noticeably closer to the $[PMo_{12}O_{40}]^{3-}$ trianions than those observed in **CD-POM-1**. Hydrogen atoms except for those involved in [C−H···O] interactions have been omitted for the sake of clarity.

observed around $q \approx 0.95$ Å^{-1}, but shifted to slightly higher q. The downturn at the low q is again a result of interparticle interactions between the complexes in the concentrated solutions. Additionally, a kink in the scattering profile at $q \approx 0.5$ Å^{-1} was noted. The low q SAXS data provide information about the size of the superstructure through the Guinier relationship, $I(q) = I_0 \exp(-q^2R_g^2/3)$, where I_0 is the absolute intensity at $q = 0$ and R_g the radius of gyration of the scattering

DOI: 10.1021/ja511713c
J. Am. Chem. Soc. 2015, 137, 4111−4118

object. Guinier analysis in the low q region (0.19−0.22 Å^{-1}) gives the radius of gyration R_g = 5.92 Å for the mixture of γ-CD and the $[PMo_{12}O_{40}]^{3-}$ trianion (inset of Figure 3c). This value is higher than R_g = 3.78 Å for the $[PMo_{12}O_{40}]^{3-}$ trianion (q = 0.29−0.31 Å^{-1}, inset of Figure 3a). The larger size found for a solution containing both CDs and POMs is consistent with the formation of 2:1 complexes. No evidence for higher order assemblies—e.g., 3:1 or 4:2 complexes—was detected by SAXS/WAXS data, as detailed in the SI.

3.5. Single-Crystal X-ray Diffraction Analyses. Both **CD-POM-1** and **CD-POM-2** exhibit a similar 2:1 sandwich-type structure wherein each $[PMo_{12}O_{40}]^{3-}$ trianion is encapsulated by the primary (1°) faces of two γ-CD (Figure 4) or β-CD (Figure 5) tori and associated through multiple intermolecular [C−H···O] hydrogen-bonding interactions.[21] This observation is in good agreement with the investigations of the complex formation observed in aqueous solution by the ^{1}H NMR titration experiments and SAXS/WAXS analyses. In both crystal structures, the hydrated $[La(H_2O)_9]^{3+}$ countercations were found outside the CD channels and stabilized through electrostatic and hydrogen-bonding interactions. Remarkably, in the case of γ-CD, the cation−anion distance is very long ($d_{P\cdots La}$ = 14 Å), an observation that can be related to the strong noncovalent association between γ-CD and the $[PMo_{12}O_{40}]^{3-}$ trianion which results in a shielding effect imposed upon the charge on the POM. In **CD-POM-1** (Figure 4a−c), the large cavity of ca. 9.5 Å diameter of γ-CD allows a deep embedding of the $[PMo_{12}O_{40}]^{3-}$ trianion, which is stabilized by three [C−H···O═Mo] interactions (closest $d_{C-H\cdots O=Mo}$ = 1.98 Å, $d_{C\cdots O=Mo}$ = 2.92 Å, $\angle_{C-H\cdots O=Mo}$ = 156°) between three of the eight H-5's of the γ-CD and three engulfed terminal O atoms (Mo═O) in the $[PMo_{12}O_{40}]^{3-}$ trianion. This superstructure is also stabilized by additional [C−H···O═Mo] interactions (closest $d_{C\cdots O=Mo}$ = 3.01 Å) between H-6/6′ protons of CD and the six "equatorial" terminal oxygen atoms in the POM. Similar interactions bolster the association between the $[PMo_{12}O_{40}]^{3-}$ trianion and a second γ-CD host (closest $d_{C-H\cdots O=Mo}$ = 2.13 Å, $d_{C\cdots O=Mo}$ = 3.07 Å, $\angle_{C-H\cdots O=Mo}$ = 154°), resulting in a 2:1 complex, which confirms our findings in the solution phase. It is noteworthy that this type of hydrogen-bonding interaction seems to be especially strong on account of the partial negative charges on the oxyanions in the POMs.

In contrast, in the solid-state superstructure of **CD-POM-2** (Figure 5a−c), only one of the terminal O atoms of the $[PMo_{12}O_{40}]^{3-}$ trianion can be embedded successfully into the cavity and so become involved in a [C−H···O═Mo] interaction ($d_{C-H\cdots O=Mo}$ = 2.25 Å, $d_{C\cdots O=Mo}$ = 3.18 Å, $\angle_{C-H\cdots O=Mo}$ = 153°) with one of the seven H-5, as a result of the smaller cavity of ca. 7.8 Å diameter and the C_7 symmetry of β-CD. Such weaker interactions can readily yield to the electrostatic interactions between the $[PMo_{12}O_{40}]^{3-}$ trianion and the $[La(H_2O)_9]^{3+}$ countercation. The much closer ($d_{P\cdots La}$ = 9.7 Å) ion-pair distance found in the single-crystal superstructure favors a somewhat bent 2:1 complex instead of a linear ternary complex.[22] The extent of complementarity between the CDs and the POM revealed in the solid-state superstructures of **CD-POM-1** and **CD-POM-2** correlates well with the relative binding affinities measured in solution phase, an observation which indicates the importance of preorganization in the molecular recognition process.

Furthermore, in both **CD-POM-1** and **CD-POM-2**, the OH groups on the secondary (2°) faces of the CDs, which are not engaged in interactions with the $[PMo_{12}O_{40}]^{3-}$ trianion, allow the tight conjunction of the 2:1 complexes to form infinite 1D bamboo-like superstructures[9b] as a result of multiple [O−H···O] hydrogen-bonding interactions[23] (mean $d_{O\cdots O}$ = 2.9 Å) between the 2° faces of the CD tori (Figures 3d and 4d). The purities of the crystal phases of both **CD-POM-1** and **CD-POM-2** are further confirmed (Figure S5) by a good correlation between the experimental powder XRD patterns and the predicted powder XRD pattern calculated from the single-crystal diffraction data.

3.6. Electrochemistry. One of the important properties of POMs is their ability to undergo multielectron reduction with minimal structural changes.[24] This ability to act as a molecular reservoir of electrons explains the increasing interest in using them in many applications,[2,3] such as energy storage, catalysis, and artificial photosynthesis. In order to investigate the redox properties of the $[PMo_{12}O_{40}]^{3-}$ trianion encapsulated by CDs, CV experiments have been carried out. The CV of a 0.1 M aqueous solution of the $[PMo_{12}O_{40}]^{3-}$ trianion exhibits three reversible waves at +440, +340, and +150 mV, relative to Ag/AgCl (Figure 6a). Upon the addition of γ-CD, the first two

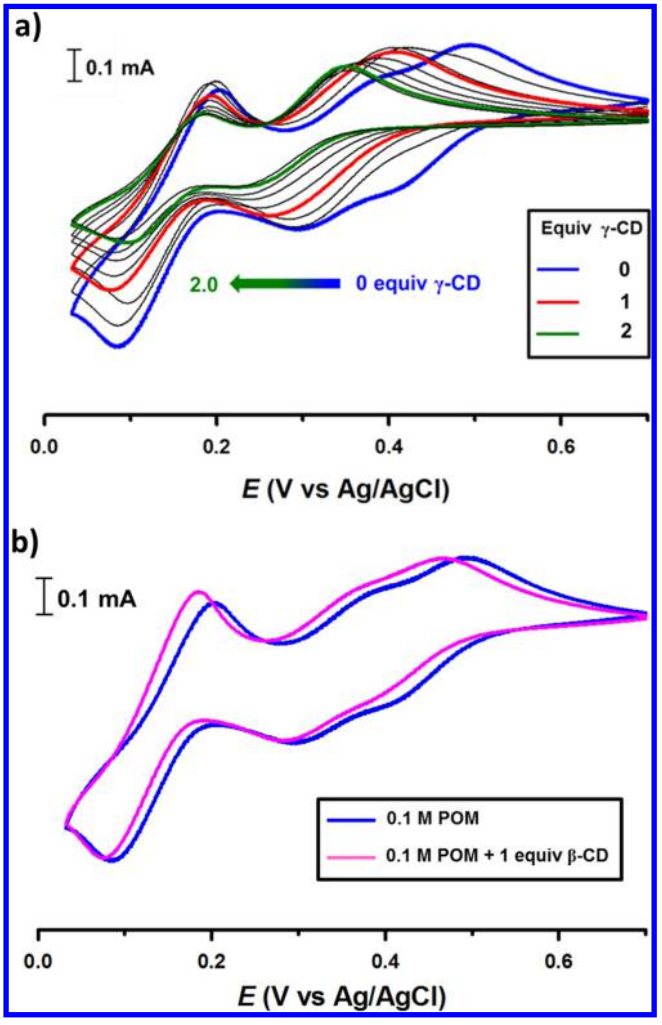

Figure 6. (a) Cyclic voltammograms (298 K, scan rate 100 mV s^{-1}) of a 0.1 M aqueous solution of the $[PMo_{12}O_{40}]^{3-}$ trianion in the presence of increasing amounts of γ-CD from 0.02 to 0.2 M. (b) Cyclic voltammograms (298 K, scan rate 100 mV s^{-1}) of 0.1 M aqueous solutions of the $[PMo_{12}O_{40}]^{3-}$ trianion in the absence and presence of β-CD (0.1 M).

DOI: 10.1021/ja511713c
J. Am. Chem. Soc. 2015, 137, 4111−4118

reduction peaks merge into one peak and are shifted to a lower potential at +320 mV, an observation which suggests that the complexation of the POM with γ-CD affects the redox properties of the Mo atoms within the $[PMo_{12}O_{40}]^{3-}$ trianion in aqueous media. The third reduction peak remains almost unaltered. On the other hand, the addition of β-CD causes only a marginal change to the CV (Figure 6b). Remarkably, we also observe that complexation of the $[PMo_{12}O_{40}]^{3-}$ trianion by CDs has a beneficial effect on the stabilization of the POM. In particular, **CD-POM-1** is stable in aqueous solution for weeks without any evident color change, while the native $[PMo_{12}O_{40}]^{3-}$ trianion shows a visible color change from yellow to deep green under the same conditions after just 1 day, providing evidence for the formation of blue-colored Mo(V). We attribute this complexation-induced stabilization in aqueous solution to both electronic perturbation, as observed in the CV experiments, and steric protection from atmospheric agents.

4. CONCLUSIONS

The self-assembly between γ-CD and β-CD with a native α-Keggin POM has been observed both in solution and in the solid state. The molecular recognition encoded in the remarkable complementarity of molecular structures—that is, size-fitness, preorganization, and hydrogen bonding—is the major driving force for the formation of these hybrid assemblies. Both ^{1}H NMR titration and X-ray scattering data provide evidence for the formation of complexes in solution phase. These pre-assembled complexes further self-organize into 1D tubular arrays in the solid-state superstructure, as shown by single-crystal diffraction analyses. Preliminary investigations of the redox properties of the $[PMo_{12}O_{40}]^{3-}$ trianion encapsulated in the cyclodextrins indicate that the redox properties of the trianion are largely retained, yet an additional chemical/electrochemical stabilization is observed. The construction of CD-POM complexes using functional and readily available CDs and POMs highlights a promising way to build new functional materials for catalysis, photocatalysis, and biomedical applications.

■ ASSOCIATED CONTENT

Supporting Information

Detailed synthetic procedures; crystallographic and spectroscopic (NMR, ITC, HRMS, and CV) characterization for **CD-POM-1** and **CD-POM-2**. This material is available free of charge via the Internet at http://pubs.acs.org.

■ AUTHOR INFORMATION

Corresponding Authors

*lihui@bit.edu.cn

*stoddart@northwestern.edu

Notes

The authors declare no competing financial interest.

■ ACKNOWLEDGMENTS

We thank Dr. Amy Sarjeant and Charlotte C. Stern for obtaining the X-ray crystallographic data; Dr. Saman Shafaie for the collection and analyses of the high-resolution mass spectrometric data; and Dr. Paul R. McGonigal and Dr. Andrew Sue for helpful discussions. Use of the Advanced Photon Source, an Office of Science User Facility operated for the U.S. Department of Energy (DOE) Office of Science by Argonne National Laboratory, was supported by the DOE under Contract No. DE-AC02-06CH11357. This research was supported by the NIH RO1 CA133697, and by the Defense Threat Reduction Agency HDTRA1-13-1-0046, and is part (Project 34-949) of the Joint Center of Excellence in Integrated Nanosystems (JCIN) at King Abdul-Aziz City for Science and Technology (KACST) and Northwestern University (NU). The authors thank both KACST and NU for their continued support of this research, which was also supported in part by the Argonne-Northwestern Solar Energy Research (ANSER) Center, an Energy Frontier Research Center funded by the DOE, Office of Science, Office of Basic Energy Sciences, under award no. DE-SC0001059 (Y.W. and M.R.W.). H.L. was supported by a Senior Visiting Scholarship of the State Scholarship Funding of the China Scholarship Council (CSC) and the National Science Council of the People's Republic of China (No. 21271026). Y.W. thanks the Fulbright Scholar Program for a Research Fellowship and support from a Ryan Fellowship awarded under the auspices of the NU International Institute for Nanotechnology (IIN).

■ REFERENCES

(1) (a) Lehn, J.-M. *Angew. Chem., Int. Ed.* **1988**, *27*, 89. (b) Lehn, J.-M. *Supramolecular Chemistry: Concepts and Perspectives*; Wiley VCH: Weinheim, Germany, 1995. (c) *Structure and Bonding: Molecular Self-Assembly: Organic Versus Inorganic Approaches*; Fujita, M., Ed.; Springer-Verlag: Heidelberg, 2000; p 96 and references therein. (d) Hartgerink, J. D.; Beniash, E.; Stupp, S. I. *Science* **2001**, *294*, 1684. (e) *Structure and Bonding: Molecular Machines and Motors*; Sauvage, J.-P., Ed.; Springer-Verlag: Heidelberg, 2001; p 99 and references therein. (f) Whitesides, G. M.; Boncheva, M. *Proc. Natl. Acad. Sci. U.S.A.* **2002**, *99*, 4769. (g) Seidel, S. R.; Stang, P. J. *Acc. Chem. Res.* **2002**, *35*, 972. (h) Lee, C.-F.; Leigh, D. A.; Pritchard, R. G.; Schultz, D.; Teat, S. J.; Timco, G. A.; Winpenny, R. E. P. *Nature* **2009**, *458*, 314. (i) Sofos, M.; Goldberger, J.; Stone, D. A.; Allen, J. E.; Ma, Q.; Herman, D. J.; Tsai, W.-W.; Lauhon, L. J.; Stupp, S. I. *Nat. Mater.* **2009**, *8*, 68. (j) Ballesteros, B.; Faust, T. B.; Lee, C.-F.; Leigh, D. A.; Muryn, C. A.; Pritchard, R. G.; Schultz, D.; Teat, S. J.; Timco, G. A.; Winpenny, R. E. P. *J. Am. Chem. Soc.* **2010**, *132*, 15435. (k) Chatterjee, T.; Sarma, M.; Das, S. K. *Cryst. Growth Des.* **2010**, *10*, 3149. (l) Gao, C.-Y.; Zhao, L.; Wang, M.-X. *J. Am. Chem. Soc.* **2011**, *133*, 8448. (m) Yu, L.; Li, M.; Zhou, X.-P.; Li, D. *Inorg. Chem.* **2013**, *52*, 10232. (n) Weingarten, A. S.; Kazantsev, R. V.; Palmer, L. C.; McClendon, M.; Koltonow, A. R.; Samuel, A. P. S.; Kiebala, D. J.; Wasielewski, M. R.; Stupp, S. I. *Nat. Chem.* **2014**, *6*, 964.

(2) (a) Cölfen, H.; Mann, S. *Angew. Chem., Int. Ed.* **2003**, *42*, 2350. (b) Sanchez, C.; Arribart, H.; Giraud Guille, M. M. *Nat. Mater.* **2005**, *4*, 277. (c) Ludlow, R. F.; Otto, S. *Chem. Soc. Rev.* **2008**, *37*, 101. (d) Nitschke, J. R. *Nature* **2009**, *462*, 736. (e) Vicens, J.; Vicens, Q. *J. Incl. Phenom. Macrocycl. Chem.* **2011**, *71*, 251. (f) Cutler, J. I.; Zhang, K.; Zheng, D.; Auyeung, E.; Prigodich, A. E.; Mirkin, C. A. *J. Am. Chem. Soc.* **2011**, *133*, 9254. (g) Miras, H. N.; Yan, J.; Long, D.-L.; Cronin, L. *Chem. Soc. Rev.* **2012**, *41*, 7403. (h) Cook, T. R.; Vajpayee, V.; Lee, M. H.; Stang, P. J.; Chi, K. W. *Acc. Chem. Res.* **2013**, *46*, 2464. (i) Miras, H. N.; Vila-Nadal, L.; Cronin, L. *Chem. Soc. Rev.* **2014**, *43*, 5679. (j) Walde, P.; Umakoshi, H.; Stano, P.; Mavelli, F. *Chem. Commun.* **2014**, *50*, 10177. (k) Brodin, J. D.; Carr, J. R.; Sontz, P. A.; Tezcan, F. A. *Proc. Natl. Acad. Sci. U.S.A.* **2014**, *111*, 2897. (l) Mattia, E.; Otto, S. *Nat. Nanotechnol.* **2015**, *10*, 111. (m) Taylor, E. *Philos. Stud.* **2015**, *172*, 653.

(3) (a) Pope, M. T.; Müller, A. *Angew. Chem., Int. Ed. Engl.* **1991**, *30*, 34. (b) Wassermann, K.; Dickman, M. H.; Pope, M. T. *Angew. Chem., Int. Ed. Engl.* **1997**, *36*, 1445. (c) Hill, C. L. *Chem. Rev.* **1998**, *98*, 1. (d) Coronado, E.; Gomez-Garcia, C. J. *Chem. Rev.* **1998**, *98*, 273. (e) Wu, C. D.; Lu, C. Z.; Zhuang, H. H.; Huang, J. S. *J. Am. Chem. Soc.* **2002**, *124*, 3836. (f) Liu, T. B.; Diemann, E.; Li, H. L.; Dress, A. W. M.; Müller, A. *Nature* **2003**, *426*, 59. (g) Peng, Z. H. *Angew Chem., Int. Ed.* **2004**, *43*, 930. (h) Mizuno, N.; Yamaguchi, K.; Kamata, K. *Coord.*

DOI: 10.1021/ja511713c
J. Am. Chem. Soc. 2015, 137, 4111−4118

Chem. Rev. **2005**, *249*, 1944. (i) Mal, S. S.; Kortz, U. *Angew. Chem., Int. Ed.* **2005**, *44*, 3777. (j) Zheng, P. Q.; Ren, Y. P.; Long, L. S.; Huang, R. B.; Zheng, L. S. *Inorg. Chem.* **2005**, *44*, 1190. (k) Hill, C. L. *J. Mol. Catal. A: Chem.* **2007**, *262*, 2. (l) Ritchie, C.; Ferguson, A.; Nojiri, H.; Miras, H. N.; Song, Y.-F.; Long, D.-L.; Burkholder, E.; Murrie, M.; Koegerler, P.; Brechin, E. K.; Cronin, L. *Angew. Chem., Int. Ed.* **2008**, *47*, 5609. (m) Proust, A.; Matt, B.; Villanneau, R.; Guillemot, G.; Gouzerh, P.; Izzet, G. *Chem. Soc. Rev.* **2012**, *41*, 7605. (n) Cronin, L.; Müller, A. *Chem. Soc. Rev.* **2012**, *41*, 7333.

(4) (a) Rhule, J. T.; Hill, C. L.; Judd, D. A. *Chem. Rev.* **1998**, *98*, 327. (b) Gao, G.; Li, F.; Xu, L.; Liu, X.; Yang, Y. *J. Am. Chem. Soc.* **2008**, *130*, 10838. (c) Yin, Q.; Tan, J. M.; Besson, C.; Geletii, Y. V.; Musaev, D. G.; Kuznetsov, A. E.; Luo, Z.; Hardcastle, K. I.; Hill, C. L. *Science* **2010**, *328*, 342. (d) Kamata, K.; Yonehara, K.; Nakagawa, Y.; Uehara, K.; Mizuno, N. *Nat. Chem.* **2010**, *2*, 478. (e) Dolbecq, A.; Dumas, E.; Mayer, C. R.; Mialane, P. *Chem. Rev.* **2010**, *110*, 6009. (f) Ettedgui, J.; Posner, Y. D.; Weiner, L.; Neumann, R. *J. Am. Chem. Soc.* **2011**, *133*, 188. (g) Stracke, J. J.; Finke, R. G. *J. Am. Chem. Soc.* **2011**, *133*, 14872. (h) Symes, D. M.; Cronin, L. *Nat. Chem.* **2013**, *5*, 403. (i) Vickers, J. W.; Lv, H. J.; Sumliner, J. M.; Zhu, G. B.; Luo, Z.; Musaev, D. G.; Geletii, Y. V.; Hill, C. L. *J. Am. Chem. Soc.* **2013**, *135*, 14110. (j) Stephanopoulos, N.; Freeman, R.; North, H. A.; Sur, S.; Jeong, S. J.; Tantakitti, F.; Kessler, J. A.; Stupp, S. I. *Nano Lett.* **2014**, *15*, 603.

(5) Sartorel, A.; Bonchio, M.; Campagna, S.; Scandola, F. *Chem. Soc. Rev.* **2013**, *42*, 2262.

(6) (a) An, H. Y.; Wang, E. B.; Xiao, D. R.; Li, Y. G.; Su, Z. M.; Xu, L. *Angew. Chem., Int. Ed.* **2006**, *45*, 904. (b) Long, D.-L.; Burkholder, E.; Cronin, L. *Chem. Soc. Rev.* **2007**, *36*, 105. (c) Raj, G.; Swalus, C.; Guillet, A.; Devillers, M.; Nysten, B.; Gaigneaux, E. M. *Langmuir* **2013**, *29*, 4388.

(7) (a) Zhang, Y.; Yang, X. D.; Wang, K.; Crans, D. C. *J. Inorg. Biochem.* **2006**, *100*, 80. (b) Toma, F. M.; Sartorel, A.; Iurlo, M.; Carraro, M.; Parisse, P.; Maccato, C.; Rapino, S.; Gonzalez, B. R.; Amenitsch, H.; Ros, T. D.; Casalis, L.; Goldoni, A.; Marcaccio, M.; Scorrano, G.; Scoles, G.; Paolucci, F.; Prato, M.; Bonchio, M. *Nat. Chem.* **2010**, *2*, 826. (c) Narasimhan, K.; Pillay, S.; Ahmad, N. R. B.; Bikadi, Z.; Hazai, E.; Yan, L.; Kolatkar, P. R.; Pervushin, K.; Jauch, R. *ACS Chem. Biol.* **2011**, *6*, 573. (d) Kowalewski, B.; Poppe, J.; Demmer, U.; Warkentin, E.; Dierks, T.; Ermler, U.; Schneider, K. *J. Am. Chem. Soc.* **2012**, *134*, 9768.

(8) (a) Proust, A.; Matt, B.; Villanneau, R.; Guillemot, G.; Gouzerh, P.; Izzet, G. *Chem. Soc. Rev.* **2012**, *41*, 7605. (b) Yvon, C.; Surman, A. J.; Hutin, M.; Alex, J.; Smith, B. O.; Long, D.-L.; Cronin, L. *Angew. Chem., Int. Ed.* **2014**, *53*, 3336. (c) Winter, R. S.; Cameron, J. M.; Cronin, L. *J. Am. Chem. Soc.* **2014**, *136*, 12753.

(9) (a) Li, G.; McGown, L. B. *Science* **1994**, *261*, 249. (b) Rekharsky, M. V.; Inoue, Y. *Chem. Rev.* **1998**, *98*, 1875. (c) Douhal, A. *Chem. Rev.* **2004**, *104*, 1955. (d) Wenz, G.; Han, B.-H.; Müller, A. *Chem. Rev.* **2006**, *106*, 782. (e) Sallas, F.; Darch, R. *Eur. J. Org. Chem.* **2008**, 957. (f) Harada, A.; Takashima, Y.; Yamaguchi, H. *Chem. Soc. Rev.* **2009**, *38*, 875. (g) van de Manakker, F.; Vermonden, T.; van Nostrum, C. F.; Hennink, W. E. *Biomacromolecules* **2009**, *10*, 3157. (h) Schneider, H.-J. *Angew. Chem., Int. Ed.* **2009**, *48*, 3924. (i) Chen, Y.; Liu, Y. *Chem. Soc. Rev.* **2010**, *39*, 495. (j) Harada, A.; Kobayashi, R.; Takashima, Y.; Hashidzume, A.; Yamaguchi, H. *Nat. Chem.* **2011**, *3*, 34. (k) Nakahata, M.; Takashima, Y.; Yamaguchi, H.; Harada, A. *Nat. Commun.* **2011**, *2*, 511. (l) Nalluri, S. K. M.; Voskuhl, J.; Bultema, J. B.; Boekema, E. J.; Ravoo, B. J. *Angew. Chem., Int. Ed.* **2011**, *50*, 9747. (m) Harada, A.; Takashima, Y. *Chem. Rec.* **2013**, *13*, 420. (n) Martinez, A.; Ortiz Mellet, C.; Garcia Fernandez, J. M. *Chem. Soc. Rev.* **2013**, *42*, 4746. (o) Schmidt, B. V. K. J.; Hetzer, M.; Ritter, H.; Barner-Kowollik, C. *Prog. Polym. Sci.* **2014**, *39*, 235. (p) Harada, A.; Takashima, Y.; Nakahata, M. *Acc. Chem. Res.* **2014**, *47*, 2128. (q) Ma, X.; Tian, H. *Acc. Chem. Res.* **2014**, *47*, 1971. (r) Yang, C.; Inoue, Y. *Chem. Soc. Rev.* **2014**, *43*, 4123.

(10) (a) Hapiot, F.; Tilloy, S.; Monflier, E. *Chem. Rev.* **2006**, *106*, 767. (b) Watanabe, K.; Kitagishi, H.; Kano, K. *Angew. Chem., Int. Ed.* **2013**, *52*, 6894. (c) Ramos, A. I.; Braga, T. M.; Silva, P.; Fernandes, J. A.; Claro, P. R.; Lopes, M. F. S.; Paz, F. A. A.; Braga, S. S. *CrystEngComm* **2013**, *15*, 2822.

(11) (a) Sengupta, S.; Kulkarni, A. *ACS Nano* **2013**, *7*, 2878. (b) Shi, Y.; Goodisman, J.; Dabrowiak, J. C. *Inorg. Chem.* **2013**, *52*, 9418.

(12) (a) González-Campo, A.; Hsu, S.-H.; Puig, L.; Huskens, J.; Reinhoudt, D. N.; Velders, A. H. *J. Am. Chem. Soc.* **2010**, *132*, 11434. (b) Jing, J.; Szarpak-Jankowska, A.; Guillot, R.; Pignot-Paintrand, I.; Picart, C.; Auzély-Velty, R. *Chem. Mater.* **2013**, *25*, 3867.

(13) (a) Loftsson, T.; Brewester, M. E. *J. Pharm. Sci.* **2012**, *101*, 3019. (b) Morrison, P. W. J.; Connon, C. J.; Khutoryanskiy, V. V. *Mol. Pharmaceutics* **2013**, *10*, 756. (c) Roux, M.; Sternin, E.; Fajolles, C.; Djedaíni-Pilard, F. *Langmuir* **2013**, *29*, 3677.

(14) (a) Schofield, W. C. E.; Bain, C. D.; Badyal, J. P. S. *Chem. Mater.* **2012**, *24*, 1645. (b) Zhang, X.; Li, X.; Deng, N. *Ind. Eng. Chem. Res.* **2012**, *51*, 704. (c) Liu, H.; Cai, X.; Chen, J. *Environ. Sci. Technol.* **2013**, *47*, 5835.

(15) (a) Forgan, R. S.; Smaldone, R. A.; Gassensmith, J. J.; Furukawa, H.; Cordes, D. B.; Li, Q.; Wilmer, C. E.; Botros, Y. Y.; Snurr, R. Q.; Slawin, A. M. Z.; Stoddart, J. F. *J. Am. Chem. Soc.* **2012**, *134*, 406. (b) Furukawa, Y.; Ishiwata, T.; Sugikawa, K.; Kokado, K.; Sada, K. *Angew. Chem., Int. Ed.* **2012**, *51*, 10566. (c) Wei, Y.; Han, S.; Walker, D. A.; Fuller, P. E.; Grzybowski, B. A. *Angew. Chem., Int. Ed.* **2012**, *51*, 7435. (d) Han, S.; Wei, Y.; Grzybowski, B. A. *Chem.—Eur. J.* **2013**, *19*, 11194. (e) Yoon, S. M.; Warren, S. C.; Grzybowski, B. A. *Angew. Chem., Int. Ed.* **2014**, *53*, 4437. (f) Bernini, M. C.; Fairen-Jimenez, D.; Pasinetti, M.; Ramirez-Pastor, A. J.; Snurr, R. Q. *J. Mater. Chem. B* **2014**, *2*, 766.

(16) In order to enhance the complexation of CDs and POMs, equipping POMs with aromatic moieties, suitable for association with the hydrophobic interior cavity of α-CDs and β-CD, has been reported: Izzet, G.; Ménand, M.; Matt, B.; Renaudineau, S.; Chamoreau, L.-M.; Sollogoub, M.; Proust, A. *Angew. Chem., Int. Ed.* **2012**, *51*, 487. This approach requires, however, pre-functionalization of a suitable POM substrate with covalent links, a requirement which limits the applicability of the method. Another investigation related to the complexation of POMs with macrocyclic hosts has been carried out on using cucurbit[n]uril (CB), where the POM moiety was found to interact with the exterior of CB molecule: Fang, X.; Kögerler, P.; Isaacs, L.; Uchida, S.; Mizuno, N. *J. Am. Chem. Soc.* **2009**, *131*, 432. In both these hybrid systems, however, the POMs have not been shown to interact with the cavities of CDs or CBs.

(17) ITC analysis for β-CD and $[PMo_{12}O_{40}]^{3-}$ anion complexation could not be performed on account of intensity of instrumental response and the low solubility of the β-CD. The experimental binding constant is based only on ^{1}H NMR titration experiments (Figure S9a).

(18) (a) Ducruix, A.; Guilloteau, J. P.; RiesKautt, M.; Tardieu, A. *J. Cryst. Growth.* **1996**, *168*, 28. (b) Tiede, D. M.; Zhang, R. T.; Seifert, S. *Biochemistry* **2002**, *41*, 6605.

(19) (a) Tiede, D. M.; Mardis, K. L.; Zuo, X. *Photosynth. Res.* **2009**, *102*, 267. (b) Zuo, X.; Tiede, D. M. *J. Am. Chem. Soc.* **2005**, *127*, 16. (c) Program is available upon request from X. Zuo (zuox@anl.gov) or D. M. Tiede (tiede@anl.gov).

(20) (a) Svergun, D. I. *J. Appl. Crystallogr.* **1992**, *25*, 495. (b) Svergun, D.; Barberato, C.; Koch, M. H. J. *J. Appl. Crystallogr.* **1995**, *28*, 768.

(21) Harata, K. *Chem. Rev.* **1998**, *98*, 1803.

(22) It should be noted that the 2:1 complexation between β-CD and the $[PMo_{12}O_{40}]^{3-}$ trianion could not be observed and hence established in the solution phase. We believe that the 2:1 complex is stabilized by the additional $[La(H_2O)_9]^{3+}$ countercation which acts as a linker in the solid state. The loss of this additional stabilization from the solvated countercation in the aqueous phase explains the formation of mainly the 1:1 complex.

(23) Desiraju, G. R. *Acc. Chem. Res.* **1991**, *24*, 290.

(24) (a) Tanaka, N.; Unoura, K.; Itabashi, E. *Inorg. Chem.* **1982**, *21*, 1662. (b) Unoura, K.; Tanaka, N. *Inorg. Chem.* **1983**, *22*, 2963. (c) Maeda, K.; Himeno, S.; Osakai, T.; Saito, A.; Hori, T. *J. Electroanal. Chem.* **1994**, *364*, 149. (d) Wu, Y.; Dou, Z.; Liu, Y.; Lv, G.; Pu, T.; He, X. *RSC Adv.* **2013**, *3*, 12726.

DOI: 10.1021/ja511713c
J. Am. Chem. Soc. 2015, 137, 4111−4118